INFECTION AND IMMUNITY, Apr. 2009, p. 1315–1323 Vol. 77, No. 4
0019-9567/09/$08.00+0 doi:10.1128/IAI.01473-08

Different Pathologies but Equal Levels of Responsiveness to the Recombinant F1 and V Antigen Vaccine and Ciprofloxacin in a Murine Model of Plague Caused by Small- and Large-Particle Aerosols[▽]

Richard J. Thomas,[1]* Daniel Webber,[1] Aaron Collinge,[1] Anthony J. Stagg,[1] Stephen C. Bailey,[1] Alejandro Nunez,[2] Amanda Gates,[1] Pramukh N. Jayasekera,[1] Rosa R. Taylor,[1] Steve Eley,[1] and Richard W. Titball[3]

Defence Science & Technology Laboratory (Dstl), Porton Down, Salisbury, Wiltshire, United Kingdom SP4 0JQ[1]; Veterinary Laboratories Agency, Weybridge, New Haw, Addlestone, Surrey, United Kingdom KT15 3NB[2]; and School of Biosciences, Geoffrey Pope Building, University of Exeter, Exeter, Devon, United Kingdom EX4 4QU[3]

Received 2 December 2008/Returned for modification 22 January 2009/Accepted 25 January 2009

Presently there is a significant effort to develop and evaluate vaccines and antibiotics against the potential bioterrorism agent *Yersinia pestis*. The animal models used to test these countermeasures involve the deposition of small particles within the lung. However, deliberate aerosol release of *Y. pestis* will generate both small and large inhalable particles. We report in this study that the pathogenesis patterns of plague infections caused by the deposition of 1- and 12-μm-particle aerosols of *Y. pestis* in the lower and upper respiratory tracts (URTs) of mice are different. The median lethal dose for 12-μm particles was 4.9-fold greater than that for 1-μm particles. The 12-μm-particle infection resulted in the degradation of the nasal mucosa and nasal-associated lymphoid tissue (NALT) plus cervical lymphadenopathy prior to bacteremic dissemination. Lung involvement was limited to secondary pneumonia. In contrast, the 1-μm-particle infection resulted in primary pneumonia; in 40% of mice, the involvement of NALT and cervical lymphadenopathy were observed, indicating entry via both URT lymphoid tissues and lungs. Despite bacterial deposition in the gastrointestinal tract, the involvement of Peyer's patches was not observed in either infection. Although there were major differences in pathogenesis, the recombinant F1 and V antigen vaccine and ciprofloxacin protected against plague infections caused by small- and large-particle aerosols.

In humans, *Yersinia pestis* infections present clinically as bubonic, septicemic, and pneumonic plague. The introduction of *Y. pestis* into the bloodstream by flea bites results in the characteristic lymphadenopathy of bubonic plague. Lymphatic and circulatory dissemination causes hematogenous seeding of the lungs, producing secondary pneumonia. Primary pneumonic plague arises from the inhalation of aerosols containing *Y. pestis*. Both bubonic and primary pneumonic plague can progress to septicemia, resulting in endotoxic shock during the terminal stages of infection (26, 29). There is currently a high level of interest in biodefense models of airborne diseases for the identification of virulence mechanisms and the testing of medical countermeasures. The focus is on the pneumonic forms of these diseases caused by the inhalation of small-particle aerosols.

Over the past decade, and in the context of the possible use of *Y. pestis* in bioterrorism, there has been significant interest in devising therapeutics for pneumonic plague. Antibiotics including tetracyclines, streptomycin, and chloramphenicol are used to treat pneumonic plague (5, 44). Recently, the broad-spectrum fluoroquinolone antibiotic ciprofloxacin has been proposed for postexposure prophylaxis for mass-casualty-setting plague (26). Ciprofloxacin possesses excellent pharmacokinetic properties, with high lung concentrations providing efficacy against murine pneumonic plague (11, 41, 42). Significant progress in the development of plague vaccines has been made. Vaccines containing F1 capsular polypeptide and LcrV (V) antigens protect against pneumonic plague in animal models (2, 22, 24, 27, 28, 46, 48).

All studies investigating the efficacy of therapeutics against aerosolized *Y. pestis* have used small airborne particles (typically 1 μm in diameter). However, natural and man-made methods for disseminating *Y. pestis* by the airborne route create a range of particle sizes. For example, coughing and sneezing produce particles ranging from >0.5 to <1,000 μm (35). The larger particles will rapidly decrease in size due to evaporation; however, their sizes will remain within the inhalable range for humans (<100 μm) over the relatively short distances (<2 m) required for the transmission of respiratory plague (25, 33, 34). Particle size influences the deposition site and hence disease pathology, with median lethal doses (MLDs) increasing with increased particle size (15, 16, 17, 18, 39); however, the efficacy of therapeutics has never been determined. Against this background, this study compares murine infections resulting from the differential deposition of small- or large-particle *Y. pestis* aerosols and the efficacies of the recombinant F1 and recombinant V antigen (rF1+rV) plague vaccine and ciprofloxacin.

* Corresponding author. Mailing address: Defence Science & Technology Laboratory (Dstl), Porton Down, Salisbury, Wiltshire, United Kingdom SP4 0JQ. Phone: (44) 01980 613199. Fax: (44) 01980 613284. E-mail: rjthomas@dstl.gov.uk.

▽ Published ahead of print on 2 February 2009.

MATERIALS AND METHODS

Animal care. Female BALB/c mice (Charles River Laboratories, United Kingdom) were housed with access to food and water ad libitum at an Advisory Committee on Dangerous Pathogens biological safety level 3 laboratory. Procedures were performed in accordance with the Scientific Procedures (Animals) Act of 1986 and the Codes of Practice for the Housing and Care of Animals Used in Scientific Procedures, 1989.

Bacterial culture and preparation of material for aerosol challenge. *Y. pestis* strain GB was cultured on Congo red agar plates at 28°C for 48 h, producing small (3- to 6-mm) pinkish red colonies with raised dark red centers. For aerosol exposures, blood agar base (BAB) broth cultures were shaken at 120 revolutions min^{-1} for 48 h at 28°C. The required dilutions were prepared in BAB broth in 10-ml volumes immediately prior to challenge. Three drops of antifoam 289 (Sigma-Aldrich Ltd., United Kingdom) was added to reduce foaming during aerosolization with the Collison nebulizer only.

Aerosol exposures. Groups of 10 mice were exposed, through the nose only, for a period of 10 min to aerosols generated by the Collison nebulizer or the flow-focusing aerosol generator (FFAG) according to the methodology described previously (43). Briefly, the 75-μm-diameter-orifice FFAG (Ingeniatrics Technologías, Seville, Spain) was operated under a pressure of 110,000 Pa with the bacterial suspension provided at a flow rate of 50 μl min^{-1} in an atmosphere with relative humidity of 65% ± 2.3%. In contrast, the three-jet Collison nebulizer was operated at 26 lb/in^2 (179,000 Pa) with conditioning in the piccolo of the Henderson apparatus at a relative humidity of 50% ± 3.7%. Both aerosols were maintained at a constant temperature of 20 ± 0.5°C and fed into a 10-port exposure tube before passing back into the Henderson apparatus through a particle analyzer (environmental dust monitor no. 107; Grimm Aerosol Technik GmbH & Co., Germany). Aerosol samples were collected for 1 min into an all-glass impinger (AGI-30; Ace Glass Inc., NJ) containing 10 ml of phosphate-buffered saline (PBS) at a flow rate of 12 liters min^{-1}. The impinger samples were serially diluted and plated onto agar for enumeration. All exposures were performed within a rigid unplasticized polyvinylchloride half-suit isolator in the biosafety level 3 laboratory. The mass median aerosol diameters of the particles from the Collison nebulizer and the FFAG were 1 to 3 μm and 12 μm, respectively. Collison nebulizer and FFAG aerosols were maintained at a constant temperature of 20 ± 0.5°C and relative humidities of 45% ± 4.1% and 65% ± 2.3%, respectively. The mean calculated inhaled dose of small particles was determined using the impinger data and Guyton's formula (23). The actual mean inhaled dose of small or large particles was determined by physical washing or dissection and homogenization of the nasal passages, trachea, and lungs as described below.

Deposition and infection kinetics. At specific time points, five mice were killed by the intraperitoneal administration of 0.5 ml of sodium pentobarbital. The tissue samples aseptically collected and homogenized in PBS were from the lungs, trachea, esophagus, stomach, intestine, liver, kidneys, and blood. Nasal washings were collected by inserting a catheter (outer and inner diameters, 1.02 and 0.58 mm, respectively; Harvard Apparatus) into a tracheal incision; material deposited in the nasal passages was washed through the nostrils by a 1-ml solution of PBS containing final concentrations of 1 mM NaOH and 0.1% (vol/vol) Triton X-100. Bacteria were enumerated by serial dilution and the plating of aliquots in triplicate onto agar plates.

Determination of the MLD. Groups of 10 mice were challenged with aerosolized *Y. pestis* bacteria at five different 10-fold dilutions via either the Collison nebulizer or the FFAG. The initial concentrations used for challenge were 10^9, 10^8, 10^7, 10^6, and 10^5 CFU ml^{-1}. These concentrations equated to retained doses of 10^4, 10^3, 10^2, 10, and 1 CFU within the lungs and nasal passages for the Collison nebulizer and the FFAG, respectively. Mice were monitored for 15 days postexposure for signs of infection. Mice showing signs of infection were killed by cervical dislocation at defined humane end points. The MLD was calculated by the 50% end point method (38), based on the numbers of bacteria retained in the lungs or nasal passages of animals that received the neat suspension. Immediately after exposure, five animals per dose were sacrificed for necroscopy, with the removal of the lungs and tracheas. The nasal passages were washed as described previously. The number of bacteria retained in the lungs or nasal passages was demonstrated to decrease by 1 logarithm with each logarithmic dilution of the spray suspension used in the dilution series.

Histopathology. Animals were dissected to expose the abdominal and thoracic cavities. The lungs were inflated by the instillation of 1.5 ml of 10% (vol/vol) neutral buffered formalin. The whole animal was fixed in 10% (vol/vol) neutral buffered formalin for 6 days, with the replacement of the formalin by a fresh aliquot after 3 days. After a further 3 days of fixation, a spleen obtained from an animal killed at 96 h postinfection was homogenized, washed, and centrifuged (7,500 × *g* for 15 min) to remove excess formalin. The resultant pellet was resuspended in BAB broth and plated to demonstrate tissue sterility. Samples from a range of tissues, including lungs (apical, medium, and caudal lobes), lymph nodes (mediastinal, cervical, inguinal, and mesenteric nodes), and the nasal cavity (including nasal-associated lymphoid tissues [NALT] and turbinates), pharynx, trachea, thymus, esophagus, stomach, intestine, jejunum (containing Peyer's patches), spleen, liver, kidneys, and sternal bone marrow, were blocked and embedded in paraffin wax. Serial 4-μm-thick sections were cut using an RM2025 microtome (Leica Microsystems Ltd., United Kingdom) and dried onto a slide at 37°C overnight. Sections were stained with hematoxylin and eosin or Gram Twort before examination using a Leica DM4000B microscope. Images were taken using a DFC480 digital camera (Leica Microsystems Ltd., United Kingdom). Animals were evaluated on the basis of the number displaying the particular type of pathology and the severity of pathology. The severity of pathology of the particular tissue was scored as −, +, +++, and +++++, equating to none, mild, marked, and severe, respectively.

Immunohistochemical detection of cleaved caspase-3. Briefly, 4-μm-thick sections were hydrated and incubated with hydrogen peroxide block (BDH Laboratory Supplies, United Kingdom), and antigen retrieval in 10 mM citrate retrieval buffer (pH 6.0) was carried out for three 6-min periods at 100°C in a microwave, prior to cooling for 10 min at room temperature. The slides were washed three times using a mixture of 50 mM Tris-buffered saline and 0.05% (vol/vol) Tween 20 (TBST [pH 8.0]; Sigma Aldrich Ltd., United Kingdom) prior to the addition of an avidin-biotin blocking system (Dako North America Inc., CA) for 10 min at room temperature. Samples were successively incubated for 60 min at room temperature with normal goat serum block, primary antibody (rabbit anti-cleaved caspase-3 antibody; Cell Signaling Technology, United Kingdom) at a 1:100 dilution in TBST, goat anti-rabbit secondary antibody (Vector Laboratories Inc.) at a 1:100 dilution in TBST, avidin-biotin-peroxidase conjugate from a Vectastain Elite ABC kit (Vector Laboratories Inc.), and 3,3′-diaminobenzidine tetrahydrochloride from an enhanced liquid substrate system (Sigma-Aldrich Ltd., United Kingdom). Three TBST rinses were performed between steps. Sections were counterstained with Meyer's hematoxylin (Surgipath, United Kingdom) and mounted before examination as described previously.

Immunization of mice with the rF1+rV plague vaccine. The vaccine formulation used in this study comprised rF1 and rV with aluminum hydroxide gel (Alhydrogel) as the adjuvant. Mice were split into two cohorts of 30 comprising three groups of 10: an unimmunized control group, an immunized neat group (given a sample of undiluted culture), and an immunized −1-dilution group. Mice in the neat and −1-dilution groups were immunized with 1 μg of each vaccine subunit formulated by coadsorption to 1.3% (vol/vol) aluminum hydroxide gel (0.26% final concentration; Brenntag Biosector, Denmark). The vaccine dose was delivered intramuscularly by equally distributing 100 μl between the two hind limbs in a two-dose regimen (on days 0 and 21). Control mice were intramuscularly given 1.3% (vol/vol) aluminum hydroxide gel. On day 27, the mice in the two cohorts were exposed by inhalation through the nose only to an aerosol containing *Y. pestis* GB produced by either the Collison nebulizer or the FFAG.

Measurement of antibodies in sera. The sera from both nonimmunized and immunized mice were collected by tail bleeds at 24 days postimmunization. Prior to challenge, the serum immunoglobulin G (IgG), IgG1, IgG2a, and IgA concentrations in each mouse were determined by an enzyme-linked immunosorbent assay. Microtiter plates (Immulon HB; Thermo Fisher Scientific) were coated with 5 μg ml^{-1} of either F1 polysaccharide or rV in PBS by overnight incubation at 4°C. The wells were washed three times with PBS containing 0.05% (vol/vol) Tween 20 and blocked with 1% (vol/vol) skim milk solution. Murine anti-F1 146.3 and anti-V 7.3 monoclonal antibodies (0.5 μg ml^{-1}) were prepared in 1% (vol/vol) skim milk solution and added to the wells allocated for the reference standards. Serum samples were prepared in 1% (vol/vol) skim milk solution at the relevant dilution. A column acted as the negative reagent control with neither antibody nor serum added. After double serial dilutions, the sealed plates were incubated for 1 h at 37°C before being washed three times with PBS containing 0.05% (vol/vol) Tween 20. Then, anti-mouse peroxidase conjugates for IgG (Bio-Rad, United Kingdom), IgG1 and IgG2a (Sigma-Aldrich Ltd., United Kingdom), and IgA (AbD-Serotec, United Kingdom) were added at a final dilution of 1:2,000 in 1% (vol/vol) skim milk solution. The plates were incubated for 1 h at 37°C and then washed three times with PBS containing 0.05% (vol/vol) Tween 20 prior to the application of the substrate, ABTS [2,2′-azinobis(3-ethylbenzthiazoline-6-sulfonic acid)] buffer containing 0.04% (vol/vol) hydrogen peroxide. The plates were incubated for 30 min at 37°C. The results were read at 414 and 492 nm on a Multiskan Ascent photometer (Thermo

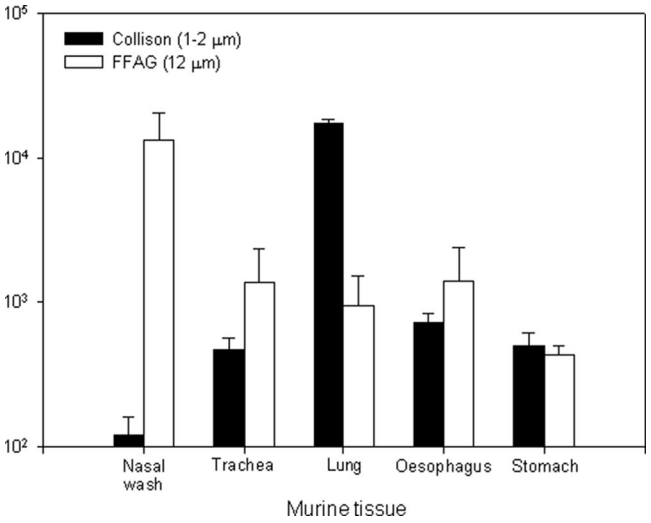

FIG. 1. Initial deposition of 1- and 12-μm-particle aerosols of *Y. pestis* GB within the murine respiratory tract at 0 h postinfection. Error bars represent the standard errors ($n = 10$).

Fisher Scientific). The IgG titers in the samples were calculated using the software ELISA for Windows (CDC).

Antibiotic efficacy. Commercially available tablets of ciprofloxacin (Bayer, United Kingdom) were dissolved in sterile distilled water to produce a final concentration of 100 mg ml^{-1}. The ciprofloxacin solutions were freshly prepared and filter sterilized prior to administration. The antibiotic dosing regimen consisted of twice-daily oral administration of 20 μl of the ciprofloxacin solution for 7 days at 12-h intervals, equating to a dose of 100 mg kg of body weight^{-1}. Groups of 10 mice were exposed to either a small- or large-particle aerosol of *Y. pestis* GB bacteria generated by the Collison nebulizer or the FFAG, respectively. The prophylactic regimen was started at either 24 or 48 h postexposure. Challenged control mice received a 7-day course of sterile distilled water. The MIC of ciprofloxacin for *Y. pestis* GB has been determined previously to be 0.025 to 0.125 mg liter^{-1} (41, 42). Survivors were humanely sacrificed by cervical dislocation 21 days postexposure. The animal tissues were processed and analyzed as described previously.

Statistical analysis. The data derived are expressed as the means and standard errors. Organs containing a bacterial load below the limit of detection (>10 CFU per organ) were designated culture negative. A two-sample *t* test was used to test the significant differences in the deposition data for the aerosols generated by the FFAG and the Collison nebulizer. The significant differences between treated and untreated groups of mice in efficacy studies were evaluated by analyses of variance followed by Tukey's honestly significant difference posttest. *P* values of <0.05 are considered to indicate significant difference.

RESULTS

Particle size influences respiratory tract deposition of *Y. pestis*. Bacteria were aerosolized using the Collison nebulizer or the FFAG to generate predominantly 1- or 12-μm-particle-size aerosols (43). These aerosols of bacteria are hereinafter referred to as 1- or 12-μm-particle aerosols. BALB/c mice were exposed to a concentration of $1.44 \times 10^9 \pm 0.26 \times 10^9$ CFU ml^{-1} within 1- or 12-μm-particle aerosols, and the site of deposition of bacteria within 30 min of exposure was determined (Fig. 1). Over 90% of the 1-μm-particle aerosol ($1.76 \times 10^4 \pm 0.085 \times 10^4$ CFU ml^{-1}) deposited in the lungs. Less than 0.6% of the bacteria ($1.2 \times 10^2 \pm 0.4 \times 10^2$ CFU ml^{-1}; $P = 0.006$) deposited in the nasal passages. Conversely, 76% of the 12-μm-particle aerosol bacteria ($1.33 \times 10^4 \pm 0.74 \times 10^4$ CFU ml^{-1}) deposited in the nasal passages, and less than 5.5% of the bacteria ($9.5 \times 10^2 \pm 5.7 \times 10^2$ CFU ml^{-1}; $P = 0.004$) were deposited in the lung tissue. Tracheal deposition patterns of bacteria were not significantly different ($P = 0.27$) for 1- and 12-μm particles. Appreciable numbers of bacteria from 1- or 12-μm particles were found in the gastrointestinal tract, constituting 6.3 and 10.5%, respectively, of the total deposited material. These results demonstrate that the bacteria in 1-μm particles deposited predominantly in the lungs and that those in 12-μm particles deposited mainly in the upper respiratory tract (URT), supporting the use of the 1- or 12-μm particles to investigate lower respiratory tract (LRT) or URT infections caused by *Y. pestis*.

Increased numbers of *Y. pestis* bacteria are required to induce an URT infection. Initially, the MLD of *Y. pestis* was determined in order to investigate the numbers of bacteria required to generate infections in the URTs and LRTs of mice challenged with 1- or 12-μm particles. A culture of *Y. pestis* containing $1.52 \times 10^9 \pm 0.04 \times 10^9$ CFU ml^{-1} was aerosolized, and the retained dose was determined. When the 1-μm-particle aerosol was generated, impinger samples indicated a retained bacterial dose of 1.90×10^4 CFU. The actual retained doses determined postmortem were 1.76×10^4 CFU in lung tissues and 90 CFU in the nasal passages. When a 12-μm-particle aerosol was generated, quantities of 7.00×10^3 and 90 CFU were recovered postmortem from the nasal passages and lungs, respectively. Tenfold serial dilutions of the initial challenge culture resulted in approximately 10-fold reductions in the numbers of bacteria deposited in the lungs or nasal passages of mice as determined by necroscopy (data not shown).

Mice with a retained dose of 10^4 CFU from 1-μm particles displayed 100% mortality, with a mean time to death (MTD) of 72 ± 0 h. Challenge with a 10-fold-lower dose resulted in protracted infection, with 40% of the mice succumbing by 120 h postinfection. No deaths occurred among mice with retained doses of 10^2 CFU or lower. When mice received a challenge with 12-μm particles producing a retained dose of 7×10^3 CFU of *Y. pestis*, 80% of the animals died, with an MTD of 90 ± 11.5 h. The remaining mice survived until the end of the experiment and cleared the infection, as evidenced by bacteriological analyses of lung and spleen tissues. Significant differences in survival rates between mice with the 1- and 12-μm-particle inhalational infections were observed at retained doses of 10^4 CFU ($P = 0.024$) and 10^3 CFU ($P = 0.001$). None of the mice challenged with 12-μm particles yielding lower retained doses died during the course of the experiment. The calculation of the MLD produced values of 601 and 2,951 CFU, respectively, for *Y. pestis* inhaled within 1- or 12-μm-particle aerosols.

Differential pathology results from the inhalation of *Y. pestis* within small- and large-particle aerosols. The temporal progression of the inhalational infections resulting from the deposition of 1- and 12-μm particles was assessed (Table 1). Differential deposition patterns in the lungs and nasal passages were achieved using the Collison nebulizer and the FFAG (Fig. 2). The inhalation of the 1-μm-particle aerosol generated by the Collison nebulizer led to the deposition of $1.23 \times 10^3 \pm 0.3 \times 10^3$ and 50 ± 20 CFU in the lungs and nasal passages, respectively. Conversely, the inhalation of the 12-μm-particle aerosol generated by the FFAG led to the deposition of 20 ± 10 and $7.09 \times 10^3 \pm 0.45 \times 10^3$ CFU in the lungs and nasal passages, respectively.

TABLE 1. Comparative histopathological progression patterns of murine inhalational plague infections in the major tissues affected

Aerosol particle size[a]	Tissue[b]	Progression of infection postchallenge[c]			
		24 h	48 h	72 h	96 h
Small (1–3 μm)	Nasal mucosa	−	+	+	+
	NALT	−	+	+++	+++
	Cervical node	−	+	+	+++[d]
	Mediastinal node	−	+	+++	+++++
	Lung	+	+++	+++++	+++++
	Spleen	−	+++	+++++	+++++
	Liver	−	+	+++	+++++
	Thymus	−	−	−	+++[d]
	Bone marrow	−	+	++	+++[d]
	Blood	−	+	+++	+++++
Large (12 μm)	Nasal mucosa	−	+++	+++++	+++++
	NALT	−	+++	+++++	+++++
	Cervical node	+	+++	+++++	+++++[d]
	Mediastinal node	−	−	−	++
	Lung	−	−	+	++
	Spleen	−	+	+	+++++
	Liver	−	−	+	+++++
	Thymus	−	−	+	+++++[d]
	Bone marrow	−	−	−	+++[d]
	Blood	−	−	+	+ + +

[a] The actual infectious doses delivered were $1.23 \times 10^3 \pm 0.3 \times 10^3$ CFU and $7.09 \times 10^3 \pm 0.45 \times 10^3$ CFU for the 1- and 12-μm-particle aerosols, respectively.

[b] Stomach, intestinal, Peyer's patch, pharyngeal, esophageal, and kidney tissues were negative for *Y. pestis* until 96 h postinfection in both 1- and 12-μm-particle inhalational infections, correlating with bacteremia. *Y. pestis* was observed only in the capillaries of these organs. Inguinal and mesenteric lymph nodes displayed pathological changes, with *Y. pestis* and neutrophils present by 48 h postinfection, in the 1-μm-particle inhalational infection. Similar pathological changes were observed only at 96 h postinfection in the 12-μm-particle inhalational infection.

[c] The severity of pathological sequelae was scored subjectively as follows: −, no sequelae; +, mild; +++, marked; and +++++, severe.

[d] Tissue where activated/cleaved caspase-3 immunolabeling was observed. Caspase-3 immunolabeling was performed only at 96 h postinfection.

The 1-μm-particle infection presented in the lungs with an initial reduction in bacterial numbers over the first 4 h before multiplication (Fig. 2a). At the terminal stages of disease, bacterial counts in the lungs exceeded 10^9 CFU g^{-1}. Histopathological analysis indicated primary pneumonia, with neutrophil infiltration and tissue consolidation evident by 48 h. At 72 to 96 h postinfection, tissue consolidation was extensive, with numerous bacteria and hemorrhages apparent within the alveoli (Fig. 3a to c). Conversely, low numbers of bacteria were deposited in the nasal passages and were rapidly cleared by 4 h postinfection, remaining below the limits of detection over the course of the experiment. Between 24 and 48 h postinfection, dissemination to other organs, including the spleen, liver, and kidneys, occurred, correlating with the onset of bacteremia. The NALT and the cervical lymph nodes (CLNs) in 30 and 40% of mice, respectively, showed involvement, with no evidence of colonization of the nasal mucosa.

Initially, the 12-μm-particle infection presented in the nasal passages, with similar numbers of bacteria retained over the course of the experiment (Fig. 2b). A transient increase in bacterial numbers in the nasal passages occurred at 48 h postinfection, correlating with the dissemination of bacteria to the lungs, spleen, and kidneys. Liver involvement associated with transient bacteremia occurred after 72 h postinfection. The bacteriological data were supported by histopathological analyses. With the exception of the CLNs, NALT, and the nasal mucosa, tissues exhibited extensive pathology only at 96 h postinfection. Lung involvement was evident only at 96 h postinfection, and the histopathology was different from that observed in the small-particle infection. Abundant bacterial colonies were closely associated with blood vessels. Severe alveolar hemorrhage was evident, with mild to minimal neutrophilic infiltration and necrosis of the pulmonary parenchyma (Fig. 3a and d to f). In all animals, ulceration of the nasal mucosa characterized by the sloughing and degeneration of ciliated epithelial cells and lymphocytic depletion within NALT were observed by 96 h postinfection; bacteria were present in both tissues (Fig. 4a and b). Neutrophil infiltration at the edges of NALT and the encapsulation of the infected tissue were noted (Fig. 4c). In some individuals, focal areas of *Y. pestis* multiplication in NALT underlying the ciliated columnar epithelium were observed (Fig. 4d). Marked histopathological changes were observed in the CLNs from animals that inhaled 12-μm particles. At 24 h postinfection, the CLNs were enlarged and hyperemic. By 96 h postinfection, complete ne-

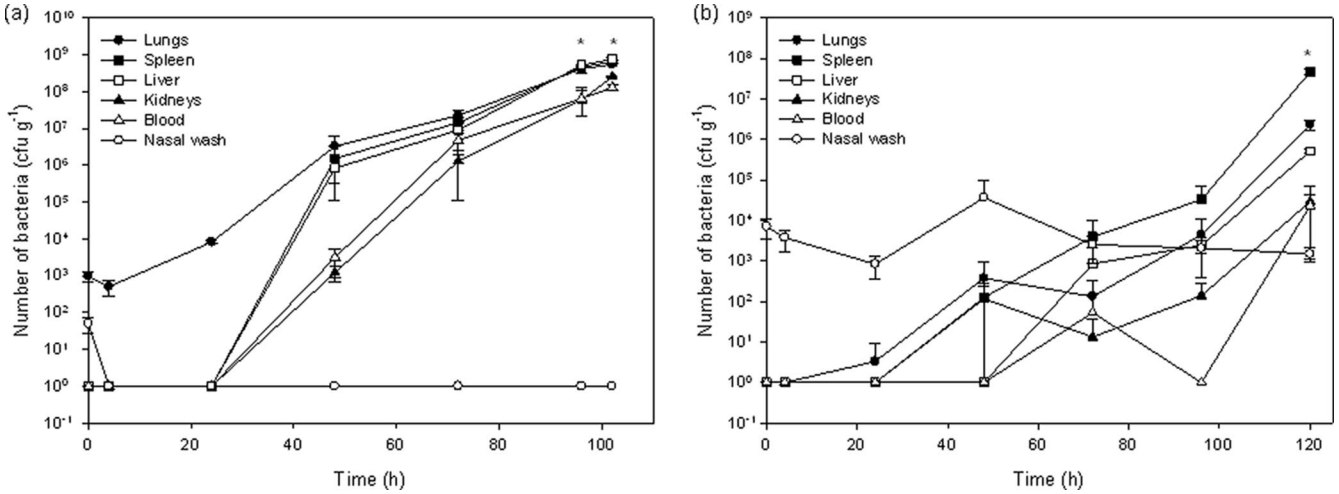

FIG. 2. Kinetics of *Y. pestis* GB aerosol infections in the murine model. Asterisks indicate time points at which deaths occurred. Error bars represent the standard errors ($n = 3$). Data are representative of results from two separate experiments. (a) Results of small (1-μm)-particle infections generated by the Collison nebulizer; (b) results of large (12-μm)-particle infections generated by the FFAG.

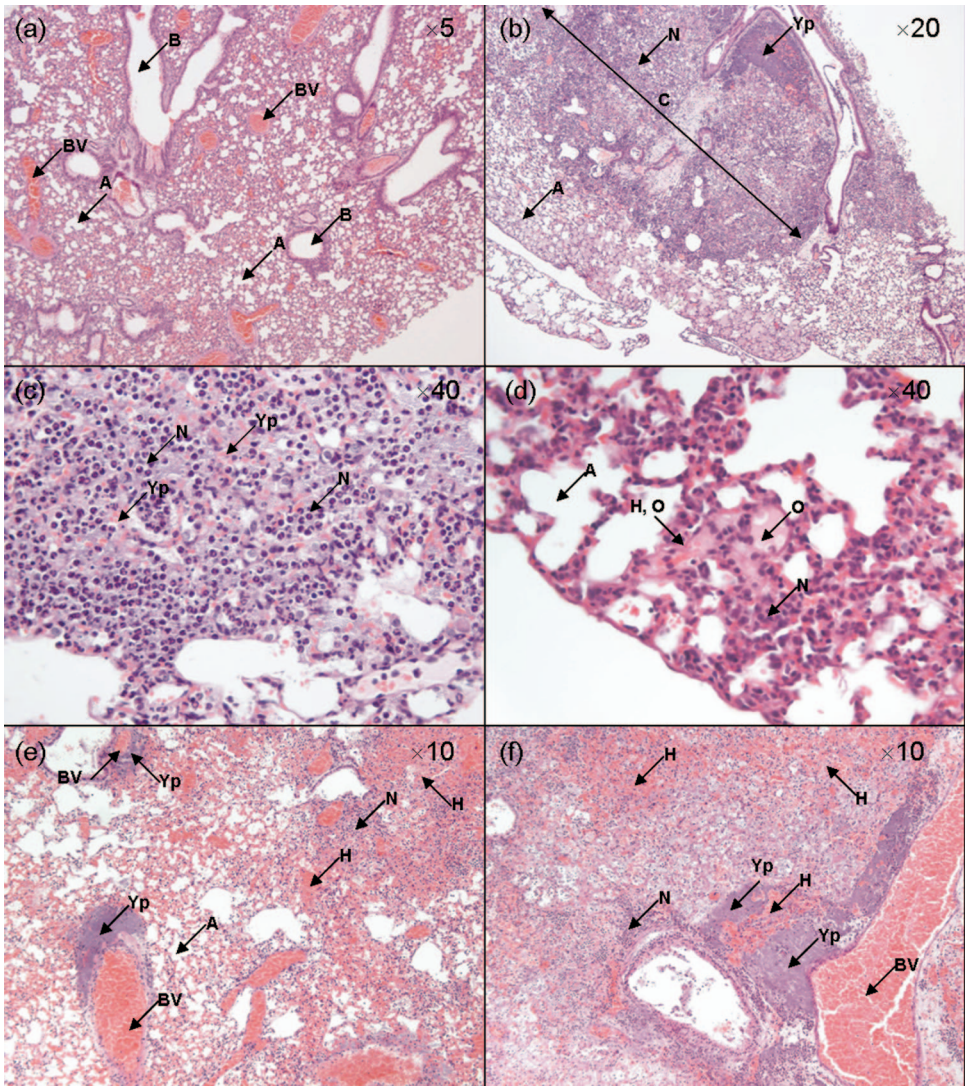

FIG. 3. Lung pathology after the inhalation of aerosolized *Y. pestis* GB. The actual infectious doses delivered were $1.23 \times 10^3 \pm 0.3 \times 10^3$ CFU and $7.09 \times 10^3 \pm 0.45 \times 10^3$ CFU for the 1- and 12-μm-particle aerosols, respectively. (a) Lung sample at 0 h postinfection (control). (b and c) Infection generated by the inhalation of 1-μm particles produced by the Collison nebulizer at 72 h postinfection. (d to f) Infection generated by the inhalation of 12-μm particles produced by the FFAG. (d) Early lesion at 72 h postinfection. (e and f) Later lesion at 96 h postinfection. Samples were stained with hematoxylin and eosin. The original magnification of each image is indicated. A, alveolar spaces; B, bronchioles; BV, blood vessels; C, consolidation of tissue; H, hemorrhage; N, neutrophils; O, edema; and Yp, *Y. pestis*.

crosis of the lymph node structure had occurred, with lymphocyte depletion and replacement by large numbers of bacteria. Pericapsular infiltration of the lymph nodes by neutrophils was observed. Infection of the CLNs occurred earlier in the 12-μm-particle inhalational infection than in the 1-μm-particle inhalational infection (Table 1).

The inhalation of 12-μm particles resulted in thymus pathology presenting as marked lymphoid depletion with the loss of differentiation between the cortex and the medulla, multifocal hemorrhages, and the presence of intravascular bacteria and numerous tingible body macrophages containing pyknotic and karyorrhectic debris. Activated/cleaved caspase-3 immunolabeling showed a very high number of lymphocytes in the thymus, indicating an accelerated apoptosis phenomenon and identifying the pyknotic and karyorrhectic debris as apoptotic bodies. Similar changes were observed in only one animal that inhaled 1-μm particles. Increased cleavage of caspase-3 in the lymphocyte populations of the sternal bone marrow and the cervical and inguinal lymph nodes was also observed at 96 h after challenge with either 1- or 12-μm-particle aerosols containing *Y. pestis*. The histopathology patterns observed in the spleen and liver were similar regardless of the size of particles inhaled; however, the changes occurred earlier in the small-particle infection, with marked pathology evident at 48 h compared to 72 to 96 h in the large-particle infection (Table 1). In both infections, terminal disease was characterized by pneumonia and septicemia at 72 to 96 h postinfection.

Efficacy of the rF1+rV vaccine against inhalational *Y. pestis* infections. An rF1+V vaccine has been shown previously to be

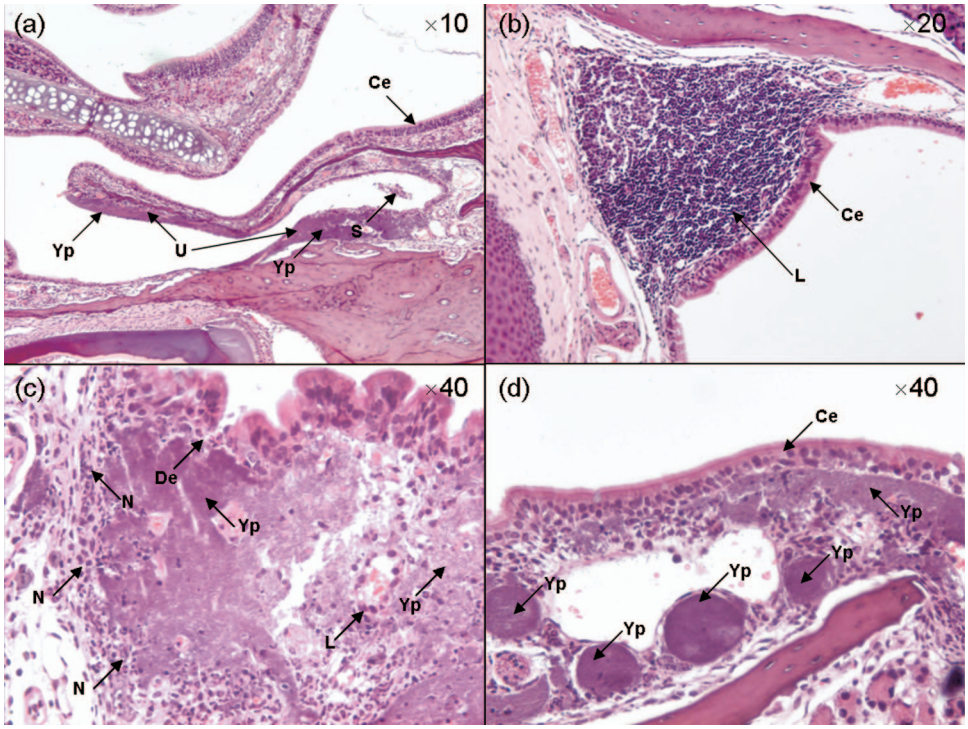

FIG. 4. Pathology of the nasal cavity after the inhalation of *Y. pestis* GB aerosolized in 12-μm particles by the FFAG. The actual infectious dose delivered was $7.09 \times 10^3 \pm 0.45 \times 10^3$ CFU. (a) Nasal turbinates and mucosa; (b) NALT at 0 h postinfection (control); (c and d) NALT at 96 h postinfection. Samples were stained with hematoxylin and eosin. The original magnification of each image is indicated. Ce, ciliated columnar epithelium; De, degraded epithelium; L, lymphocytes; N, neutrophils; S, sloughed epithelial cells; U, ulceration; and Yp, *Y. pestis*.

efficacious in protecting mice from disease caused by the inhalation of a small-particle *Y. pestis* aerosol (46, 48). In this study, the efficacy of the rF1+rV vaccine in providing protection against disease caused by the inhalation of *Y. pestis* within small or large particles was determined (Table 2). The total concentrations of the IgG and IgG1, IgG2a, and IgA subtypes in sera were determined prechallenge ($n = 40$). The sera of immunized mice had mean titers of IgG against the F1 and V antigens of 207.7 ± 34.1 and 135.2 ± 18.6 μg ml^{-1}, respectively ($P = 0.003$). The serum IgG1 and IgG2a titers were 36.92 ± 3.87 and 2.36 ± 0.23 μg ml^{-1}, respectively, for rF1 and 69.11 ± 7.12 and 0.085 ± 0.043 μg ml^{-1}, respectively, for rV. Both antigens generated greater IgG1 titers than IgG2a titers ($P = <0.05$). However, rV generated a greater IgG1 response than rF1 ($P = 0.001$), while the converse was true for the IgG2a response ($P = 0.001$). No serum IgA response was observed for either the F1 or the V antigen. The mice were exposed to 5.5 MLDs of *Y. pestis* within either small or large particles. Significant differences in survival rates ($P < 0.05$) between the control and immunized mice were observed for both types of inhalational infections. All of the control mice immunized with aluminum hydroxide gel alone and challenged with 1-μm particles containing *Y. pestis* died, with an MTD of 72 ± 0 h. Only 80% of mice that were challenged with *Y. pestis* in 12-μm particles died, with an MTD of 114 ± 8.8 h.

TABLE 2. Efficacies of rF1+rV vaccine and ciprofloxacin against inhalational plague infections caused by small or large particles

Aerosol particle size (μm)	No. of survivors/no. in group (% survival)				
	rF1+rV vaccine		Ciprofloxacin[a] (100 mg ml^{-1})		
	No rF1+rV vaccine	rF1+rV vaccine	Control (0 hpi)	24 hpi	48 hpi
1–3	0/10 (0)	10/10 (100)	0/10 (0)	10/10 (100)	9/10 (90)
12	2/10 (20)	10/10 (100)	0/10 (0)	10/10 (100)	9/10 (90)

[a] Time points indicate the hours postinfection (hpi) at which treatment was administered.

None of the immunized mice succumbed to infection, irrespective of whether *Y. pestis* was delivered in small or large particles. The clearance of *Y. pestis* from immunized animals was confirmed by the inability to culture bacteria from the lungs or spleens of the survivors at 21 days postchallenge. Histological analysis of the immunized mice did not reveal any adverse pathology associated with immunization or subsequent challenge with *Y. pestis*. Furthermore, none of the immunized mice displayed any adverse clinical signs after challenge; in contrast, control mice displayed ruffled fur and a hunched posture by 48 h postchallenge. Histological examination of nonimmunized control mice at the time of death indicated pathology characteristic of either LRT or URT infection, dependent on exposure to 1- or 12-μm particles.

Ciprofloxacin protects against small- and large-particle inhalational *Y. pestis* infections. The efficacy of ciprofloxacin in providing protection against a small-particle inhalational challenge with *Y. pestis* has been demonstrated previously (11, 40, 41, 42). Here, the efficacy of ciprofloxacin (100 mg kg^{-1}) in protecting groups of 10 mice against a lethal challenge with *Y. pestis* within either small or large particles was investigated

(Table 2). Mice were challenged with between 3.5 and 4.0 MLDs of *Y. pestis* within either 1- or 12-μm aerosol particles. The numbers of *Y. pestis* bacteria deposited in the lungs and nasal passages equated to $2.53 \times 10^3 \pm 0.28 \times 10^3$ CFU and 40 ± 20 CFU for 1-μm particles and $1.13 \times 10^2 \pm 0.07 \times 10^2$ CFU and $1.02 \times 10^4 \pm 0.55 \times 10^4$ CFU for 12-μm particles. The MTD for untreated control mice was 77.6 ± 2.5 h or 60.7 ± 3.2 h for 1- or 12-μm particles, respectively.

Antibiotic treatment commenced at either 20 or 44 h postchallenge, with a twice-daily regimen of 100 mg kg^{-1} ciprofloxacin at 12-h intervals for 7 days. Survival rates of 100 or 90%, respectively, were achieved when prophylaxis was started 20 or 44 h postchallenge, irrespective of the particle size. The clearance of *Y. pestis* from treated animals was confirmed by analyses of the lungs and spleens of the survivors. Histopathological analyses and bacteriological analyses of tissues demonstrated the typical LRT or URT pathogenesis associated with the inhalation of *Y. pestis* within 1- or 12-μm particles, respectively (data not shown). Furthermore, a remission of clinical signs over the period from 96 to 151 h in survivors from all ciprofloxacin-treated groups was observed, with mice progressing from having ruffled fur and a hunched posture to having ruffled fur only to being fully active and alert by 168 h postinfection. In the cases of both the 1- and 12-μm-particle inhalational infections, 55% of the mice that died during the course of the rF1+rV and ciprofloxacin experiments presented with eye problems such as conjunctivitis or blindness.

DISCUSSION

Humans exposed to airborne *Y. pestis* either naturally or intentionally will likely inhale both small and large particles. This is the first report of the comparative pathogenesis patterns of disease after the exposure of mice to 1- and 12-μm-particle aerosols and the efficacy of therapeutics for these different disease forms. All previous studies with mice have used small particles that penetrate into the alveoli. Recently, we reported the use of the FFAG to generate microbiological aerosols containing predominantly 12-μm particles (43). This FFAG has been used to generate large particles containing *Y. pestis.* The exposure of mice to 12-μm particles resulted in the preferential deposition of *Y. pestis* in the nasal passages of mice, whereas 1-μm particles deposited primarily within the lungs. After the exposure of mice to either 1- or 12-μm particles, bacteria could be recovered from the gastrointestinal tract. However, there was no histological evidence for infection via this route. In support of this finding, the MLD of intragastrically delivered *Y. pestis* was determined previously to be 2.09×10^6 CFU (10), a dose far exceeding the numbers entering the gastrointestinal tract in this study. Our finding that the MLD for bacteria delivered in 12-μm particles was 4.9-fold higher than that for bacteria delivered in 1-μm particles is broadly similar to the 2.5-fold difference in MLDs reported for similar particle sizes in guinea pigs (17). The MLD of 601 CFU for the 1-μm-particle aerosols is similar to MLD values ranging from 100 to 900 CFU obtained in other studies (40, 46).

The 1- and 12-μm-particle infections differed markedly (Table 1). Primary pneumonic plague developed from the deposition of 1-μm particles in the lungs, as demonstrated in previous studies (1, 9, 31). Lung involvement in the 12-μm-particle infection was limited to the terminal stages. The close proximity of *Y. pestis* to capillaries and extensive hemorrhages within the lung architecture indicated secondary pneumonia. This study presents the first evidence for the involvement of URT lymphoid tissues such as NALT and the draining lymph nodes in the pathogenesis of murine inhalational plague infections. NALT can be considered to be the equivalent of the naso-oropharyngeal lymphoid tissues present in higher mammals, including humans. These lymphoid tissues respond to the deposited antigenic challenge from inhaled or ingested material, generating specific mucosal immunity in the naso-oropharyngeal region (4, 6, 7, 30). However, as indicated in this study, they can also act as a route of infection for deposited lymphotrophic bacteria such as *Y. pestis*. Rodent NALT and human tonsillar and adenoid tissues contain M cells, dendritic cells, and macrophages (3, 4, 6, 30). Influenza A virions and group A streptococci use M cells in nasopharyngeal lymphoid tissue as a gateway (21, 36); *Y. pestis* may utilize M cells in a similar manner. The terminal stages of both the 1- and 12-μm-particle inhalational infections were characterized by systemic dissemination from the initial foci (NALT, CLNs, and/or lungs) despite attempted neutrophilic encapsulation earlier in the infection.

The induction of macrophages, lymphocytes, and dendritic cells in the apoptotic pathway is a well-characterized phenomenon during infection with *Y. pestis*. Caspase-3 is a marker of apoptotic activity, previously demonstrated to be activated in response to *Y. pestis* interaction with macrophage and T-lymphocyte cell lines (8, 32, 51). Increased numbers of lymphoid and myeloid cells possessing cleaved caspase-3 were observed in lymphoid tissues, indicating increased apoptosis. This is the first demonstration of in vivo caspase-3 activation during inhalational plague infections.

Previously, the efficacy of an rF1+rV vaccine against pneumonic plague in mice after the inhalation of 1-μm particles was demonstrated (46, 48) and attributed to protective IgG titers, with the predominance of the IgG1 isotype (2, 45, 46, 47, 48). The absence of secretory IgA and the presence of IgG in bronchial wash fluids indicated that immunity was due to a systemic immune response (45). For the first time, we demonstrate that the rF1+rV vaccine is effective in preventing disease caused by the inhalation of *Y. pestis* within large particles. The protective effect of the rF1+rV vaccine against URT challenge is due partly to the predominant serum F1- and V-specific IgG1 response elicited during immunization. The rF1+rV vaccine is currently undergoing human clinical trials. Taken with the findings of this study, the accumulative data indicate that the vaccine elicits protection against a range of *Y. pestis* infections, including bubonic and LRT and URT inhalational infections, in animal models (46, 48). Additionally, the size of the inhaled particles did not affect the efficacy of ciprofloxacin. At least 90% survival occurred when ciprofloxacin was administered up to 44 h postchallenge.

Interestingly, 55% of mice that succumbed to inhalational plague infections caused by either small or large particles presented with ocular manifestations such as blindness and conjunctivitis. Ocular plague presenting as keratoconjunctivitis with various degrees of necrotizing and fibropurulent endophthalmitis in mule deer has recently been observed. This form is not associated with morbidity or mortality (19). Ocular mani-

festation in this study was observed only at the gross level and appeared during the terminal stages of infection; hence, it is unclear whether ocular involvement was initiated through the deposition of *Y. pestis*-containing particles on the conjunctiva during aerosol exposure or through hematogenous spread via the ocular capillaries during the septicemic stage of the infections. In addition to the lower and upper respiratory mucosal surfaces, the ocular conjunctiva should be considered as a portal of entry for aerosolized pathogens to invade the body.

This study demonstrated the effectiveness of the FFAG to generate large-particle aerosols that deposit within the URTs of mice, producing an infection that differs from primary pneumonic plague. URT manifestations of plague in humans are known to include cervical lymphadenopathy, tonsillitis, peritonsillar abscesses, and pseudomembranous pharyngitis, with pulmonary involvement being limited to fulminant pneumonia (12, 13, 14, 20, 26, 34, 37, 49, 50). This form of plague may arise from the deposition of *Y. pestis* contained within large particles in the nasopharyngeal or oropharyngeal region of the URT; extrapolation from murine and guinea pig data indicates that deposition in these regions would produce infection via the URT lymphoid tissues with drainage to the CLNs, terminating in septicemia. The severity of infection would be related to the initial deposition, the clearance kinetics, and the immunological response. It is probable that the initial route of infection in patients suffering from this form of inhalational plague is often masked, and the clinical spectrum of this form of infection is worth consideration from a therapeutic perspective in the event of a bioterror attack using *Y. pestis*. Immunization using the rF1+rV vaccine or the administration of ciprofloxacin protected against the complete spectrum of inhalational infections expected upon exposure to a bioterror release of *Y. pestis*.

ACKNOWLEDGMENTS

We recognize the contribution of Ministry of Defense funding for this work.

Special thank you is reserved for the personnel involved in animal husbandry related to the completion of the experiments at Dstl Porton Down, United Kingdom. We are grateful for the expertise of the scientific and technical staff at the Histopathology Department, VLA Weybridge, United Kingdom, during the preparation and analysis of histological samples. We are grateful for the assistance of Wendy Butcher for the determination of the serum Ig titers.

REFERENCES

1. **Agar, S. L., J. Sha, S. M. Foltz, T. E. Erova, K. G. Walberg, T. E. Parham, W. B. Baze, G. Suarez, J. W. Peterson, and A. K. Chopra.** 2008. Characterization of a mouse model of plague after aerosolisation of *Yersinia pestis* CO92. Microbiology **154:**1939–1948.
2. **Anderson, G. W., Jr., S. E. Leary, E. D. Williamson, R. W. Titball, S. L. Welkos, P. L. Worsham, and A. M. Friedlander.** 1996. Recombinant V antigen protects mice against pneumonic and bubonic plague caused by F1-capsule-positive and -negative strains of *Yersinia pestis*. Infect. Immun. **64:**4580–4585.
3. **Asanuma, H., A. H. Thompson, T. Iwasaki, Y. Sato, Y. Inaba, C. Aizawa, T. Kurata, and S. Tamura.** 1997. Isolation and characterization of mouse nasal-associated lymphoid tissue. J. Immunol. Methods **202:**123–131.
4. **Bienenstock, J., and M. R. McDermott.** 2005. Bronchus- and nasal-associated lymphoid tissues. Immunol. Rev. **206:**22–31.
5. **Boulanger, L. L., P. Ettestad, J. D. Fogarty, D. T. Dennis, D. Romig, and G. Mertz.** 2004. Gentamicin and tetracyclines for the treatment of human plague: review of 75 cases in New Mexico, 1985–1999. Clin. Infect. Dis. **38:**663–669.
6. **Brandtzaeg, P., F. L. Jahnsen, I. N. Farstad, and G. Haraldsen.** 1997. Mucosal immunology of the upper airways: an overview. Ann. N. Y. Acad. Sci. **830:**1–18.
7. **Brandtzaeg, P.** 2003. Immunology of tonsils and adenoids: everything the ENT surgeon needs to know. Int. J. Pediatr. Otorhinolaryngol. **67:**S69–S76.
8. **Bruckner, S., S. Rhamouni, L. Tautz, J.-B. Denault, A. Alonso, B. Becattini, G. S. Salvesen, and T. Mustelin.** 2005. *Yersinia* phosphatase induces mitochondrially dependent apoptosis of T cells. J. Biol. Chem. **280:**10388–10394.
9. **Bubeck, S. S., A. M. Cantwell, and P. H. Dube.** 2007. Delayed inflammatory response to primary pneumonic plague occurs in both outbred and inbred mice. Infect. Immun. **75:**697–705.
10. **Butler, T., Y.-S. Fu, L. Furman, C. Almeida, and A. Almeida.** 1982. Experimental *Yersinia pestis* infection in rodents after intragastric inoculation and ingestion of bacteria. Infect. Immun. **36:**1160–1167.
11. **Byrne, W. R., S. L. Welkos, M. L. Pitt, K. J. Davis, R. P. Brueckner, J. W. Ezzell, G. O. Nelson, J. R. Vaccaro, L. C. Battersby, and A. M. Friedlander.** 1998. Antibiotic treatment of experimental pneumonic plague in mice. Antimicrob. Agents Chemother. **42:**675–681.
12. **Christie, A. B., T. H. Chen, and S. S. Elberg.** 1980. Plague in camels and goats: their role in human epidemics. J. Infect. Dis. **141:**724–726.
13. **Conrad, F. G., F. R. LeCocq, and R. Krain.** 1968. A recent epidemic of plague in Vietnam. Arch. Int. Med. **122:**193–198.
14. **Crowell, B. C.** 1915. Pathologic anatomy of bubonic plague. Philippine J. Sci. **10B:**249–308.
15. **Day, W. C., and R. F. Berendt.** 1972. Experimental tularaemia in *Macaca mulatta*: relationship of aerosol particle size to the infectivity of airborne *Pasteurella tularensis*. Infect. Immun. **5:**77–82.
16. **Druett, H. A., D. W. Henderson, L. P. Packman, and S. Peacock.** 1953. Studies on respiratory infection. I. The influence of particle size on respiratory infection with anthrax spores. J. Hyg. **51:**359–371.
17. **Druett, H. A., J. M. Robinson, D. W. Henderson, L. Packman, and S. Peacock.** 1956. The influence of aerosol particle size on infection of the Guinea-pig with *Pasteurella pestis*. J. Hyg. **54:**37–48.
18. **Druett, H. A., D. W. Henderson, and S. Peacock.** 1956. Studies on respiratory infection. III. Experiments with *Brucella suis*. J. Hyg. **54:**49–57.
19. **Edmunds, D. R., E. S. Williams, D. O'Toole, K. W. Mills, A. M. Boerger-Fields, P. T. Jaeger, R. J. Bildfell, P. Dearing, and T. E. Cornish.** 2008. Ocular plague (*Yersinia pestis*) in mule deer (*Odocoileus hemionus*) from Wyoming and Oregon. J. Wildl. Dis. **44:**983–987.
20. **Flexner, S.** 1901. The pathology of bubonic plague. Am. J. Med. Sci. **122:** 396–416.
21. **Fujimara, Y., M. Takeda, H. Ikai, K. Haruma, T. Akisada, T. Harada, T. Sakai, and M. Ohuchi.** 2004. The role of M cells of human nasopharyngeal lymphoid tissue in influenza virus sampling. Virchows Arch. **444:**36–42.
22. **Glynn, A., C. J. Roy, B. S. Powell, J. J. Adamovicz, L. C. Freytag, and J. D. Clements.** 2005. Protection against aerosolized *Yersinia pestis* challenge following homologous and heterologous prime-boost with recombinant plague antigens. Infect. Immun. **73:**5256–5261.
23. **Guyton, A.** 1947. Measurement of the respiratory volumes of laboratory animals. Am. J. Physiol. **150:**70–77.
24. **Heath, D. G., G. W. Anderson, M. Mauro, S. L. Welkos, G. P. Andrews, J. Adamovicz, and A. M. Friedlander.** 1998. Protection against experimental bubonic and pneumonic plague by a recombinant capsular F1-V antigen fusion protein vaccine. Vaccine **16:**1131–1137.
25. **Heyder, J., J. Gebhart, G. Rudolf, C. F. Schiller, and W. Stahlhofen.** 1986. Deposition of particles in the human respiratory tract in the size range 0.005–15 μm. J. Aerosol Sci. **17:**811–825.
26. **Inglesby, T. V., D. T. Dennis, D. A. Henderson, J. G. Bartlett, M. S. Ascher, E. Eitzen, A. D. Fine, A. M. Friedlander, J. Hauer, J. F. Koerner, M. Layton, J. McDade, M. T. Osterholm, T. O'Toole, G. Parker, T. M. Perl, P. K. Russell, M. Schoch-Spana, and K. Tonat.** 2000. Plague as a biological weapon—medical and public health management. JAMA **283:**2281–2290.
27. **Jones, S. M., F. Day, A. J. Stagg, and R. W. Titball.** 2001. Protection conferred by a fully recombinant sub-unit vaccine against *Yersinia pestis* in male and female mice of four inbred strains. Vaccine **19:**358–366.
28. **Jones, T., J. J. Adamovicz, S. L. Cyr, C. R. Bolt, N. Bellerose, L. M. Pitt, G. H. Lowell, and D. S. Burt.** 2006. Intranasal Protollin/F1-V vaccine elicits respiratory and serum antibody responses and protects mice against lethal aerosolized plague infection. Vaccine **24:**1625–1632.
29. **Krishna, G., and R. Chitkara.** 2003. Pneumonic plague. Semin. Respir. Infect. **18:**159–167.
30. **Kuper, C. F., P. J. Koornstra, D. M. H. Hameleers, J. Biewenga, B. J. Spit, A. M. Duijvestijn, P. J. C. van Breda Vriesman, and T. Sminia.** 1992. The role of nasopharyngeal lymphoid tissue. Immunol. Today **13:**219–224.
31. **Lathem, W. W., S. D. Crosby, V. L. Miller, and W. E. Goldman.** 2005. Progression of primary pneumonic plague: a mouse model of infection, pathology, and bacterial transcriptional activity. Proc. Natl. Acad. Sci. USA **102:**17786–17791.
32. **Marketon, M. M., R. W. DePaolo, K. L. DeBord, B. Jabri, and O. Schneewind.** 2005. Plague bacteria target immune cells during infection. Science **309:**1739–1741.
33. **Menache, M., F. Miller, and O. Raabe.** 1995. Particle inhalability curves for humans and small laboratory animals. Ann. Occup. Hyg. **39:**317–328.
34. **Meyer, K. F.** 1961. Pneumonic plague. Bacteriol. Rev. **25:**249–261.
35. **Nicas, M., W. W. Nazaroff, and A. Hubbard.** 2005. Toward understanding the risk of secondary airborne infection: emission of respirable pathogens. J. Occup. Environ. Hyg. **2:**143–154.

36. **Park, H.-S., K. P. Francis, J. Yu, and P. P. Cleary.** 2003. Membranous cells in nasal-associated lymphoid tissue: a portal of entry for the respiratory mucosal pathogen group A streptococcus. J. Immunol. **171:**2532–2537.
37. **Pollitzer, R., and C. C. Li.** 1943. Some observations on the decline of pneumonic plague epidemics. J. Infect. Dis. **72:**160–162.
38. **Reed, L. J., and H. Muench.** 1938. A simple method of estimating fifty per cent endpoints. Am. J. Hyg. **27:**493–497.
39. **Roy, C. J., M. Hale, J. M. Hartings, L. Pitt, and S. Duniho.** 2003. Impact of inhalation exposure modality and particle size on the respiratory deposition of ricin in Balb/c mice. Inhal. Toxicol. **15:**619–638.
40. **Russell, P., S. M. Eley, S. E. Hibbs, R. J. Manchee, A. J. Stagg, and R. W. Titball.** 1995. A comparison of plague vaccine USP and EV76 vaccine induced protection against *Yersinia pestis* in a murine model. Vaccine **13:**1551–1556.
41. **Russell, P., S. M. Eley, M. Green, A. J. Stagg, R. R. Taylor, M. Nelson, R. J. Beedham, D. L. Bell, D. Rogers, D. Whittington, and R. W. Titball.** 1998. Efficacy of doxycycline and ciprofloxacin against experimental *Yersinia pestis* infection. J. Antimicrob. Chemother. **41:**301–305.
42. **Steward, J., M. S. Lever, P. Russell, R. J. Beedham, A. J. Stagg, R. R. Taylor, and T. J. Brooks.** 2004. Efficacy of the latest fluoroquinolones against experimental *Yersinia pestis*. Int. J. Antimicrob. Agents **24:**609–612.
43. **Thomas, R. J., D. Webber, W. Sellors, A. Collinge, A. Frost, A. J. Stagg, S. C. Bailey, P. N. Jayasekera, R. R. Taylor, S. Eley, and R. W. Titball.** 2008. Characterization and deposition of respirable large- and small-particle bioaerosols. Appl. Environ. Microbiol. **74:**6437–6443.
44. **WHO Expert Committee on Plague.** 1970. Fourth report. World Health Organ. Tech. Rep. Ser. **447:**1–25.
45. **Williamson, E. D., S. M. Eley, K. F. Griffin, M. Green, P. Russell, S. E. Leary, P. C. Oyston, T. Easterbrook, K. M. Reddin, A. Robinson, and R. W. Titball.** 1995. A new improved sub-unit vaccine for plague: the basis of protection. FEMS Immunol. Med. Microbiol. **12:**223–230.
46. **Williamson, E. D., S. M. Eley, A. J. Stagg, M. Green, P. Russell, and R. W. Titball.** 1997. A sub-unit vaccine elicits IgG in serum, spleen cell cultures and bronchial washings and protects immunised animals against pneumonic plague. Vaccine **15:**1079–1084.
47. **Williamson, E. D., P. M. Vesey, K. J. Gillhespy, S. M. Eley, M. Green, and R. W. Titball.** 1999. An IgG1 titre to the F1 and V antigens correlates with protection against plague in the mouse model. Clin. Exp. Immunol. **116:**107–114.
48. **Williamson, E. D., A. J. Stagg, S. M. Eley, R. Taylor, M. Green, S. M. Jones, and R. W. Titball.** 2007. Kinetics of the immune response to (F1+V) vaccine in models of bubonic and pneumonic plague. Vaccine **25:**1142–1148.
49. **Worsham, P. L., T. W. McGovern, N. J. Vietri, and A. M. Friedlander.** 2007. Plague, p. 91–120. *In* D. F. Zembek (ed.), Medical aspects of biological warfare. TMM Publications, Washington, DC.
50. **Wu, L.-T., J. W. H. Chun, and R. Pollitzer.** 1922. Clinical observations upon the second Manchurian plague epidemic, 1920–1921. Nat. Med. J. China **8:**225–255.
51. **Zhang, Y., and J. B. Bliska.** 2005. Role of macrophage apoptosis in the pathogenesis of *Yersinia*. Curr. Top. Microbiol. Immunol. **289:**151–174.

Editor: J. B. Bliska